CCFE
CULHAM CENTRE FOR FUSION ENERGY

UK Atomic Energy Authority

UKAEA-CCFE-PR(24)02

K. K. KIROV, F. AURIEMMA, P. J. BONOFIGLO, C. D. CHALLIS, E. DE LA LUNA, J. ERIKSSON, D. GALLART, J. GARCIA, M. GORELENKOVA, J. HOBIRK, P. JACQUET, A. KAPPATOU, Y. KAZAKOV, D. KEELING, D. KING, V. KIPTILY, et al.

"Analysis of Fusion Alphas Interaction with RF Waves in D-T Plasma at JET

“Analysis of Fusion Alphas Interaction with RF Waves in D-T Plasma at JET

K. K. KIROV, F. AURIEMMA, P. J. BONOFIGLO, C. D. CHALLIS, E. DE LA LUNA, J. ERIKSSON, D. GALLART, J. GARCIA, M. GORELENKOVA, J. HOBIRK, P. JACQUET, A. KAPPATOU, Y. KAZAKOV, D. KEELING, D. KING, V. KIPTILY, et al.

This is a preprint of a paper submitted for publication in Nuclear Fusion

ANALYSIS OF FUSION ALPHAS INTERACTION WITH RF WAVES IN D-T PLASMA AT JET

K. K. KIROV[1], F. AURIEMMA[2], P. J. BONOFIGLO[3], C. D. CHALLIS[1], E. DE LA LUNA[4], J. ERIKSSON[5], D. GALLART[6], J. GARCIA[7], M. GORELENKOVA[3], J. HOBIRK[8], P. JACQUET[1], A. KAPPATOU[8], Y. KAZAKOV[9], D. KEELING[1], D. KING[1], V. KIPTILY[1], E. LERCHE[9], C. MAGGI[1], J. MAILLOUX[1], M. MASLOV[1], M. MANTSINEN[6], P. MANTICA[10], S. MENMUIR[1], R. SHARMA[1], P. SIREN[1], Z. STANCAR[1], D. VAN EESTER[9] AND JET CONTRIBUTORS*

[1] UKAEA (United Kingdom Atomic Energy Authority), Culham Science Centre, Abingdon, Oxfordshire, OX14 3DB, UK
[2] Consorzio RFX ISTP-CNR, 35127 Padova, Italy
[3] PPPL, Princeton University, Princeton NJ 08543-0451, USA
[4] Laboratorio Nacional de Fusión, CIEMAT, 28040 Madrid, Spain
[5] Department of Physics and Astronomy, Uppsala University, SE-75120 Uppsala, Sweden
[6] Barcelona Supercomputing Center, Barcelona, Spain
[7] CEA, IRFM, F-13108 St-Paul-Lez-Durance, France
[8] Max-Planck-Institut für Plasmaphysik, Boltzmannstr. 2, 85748 Garching, Germany
[9] Laboratory for Plasma Physics, ERM/KMS, B-1000 Brussels, Belgium
[10] Institute of Plasma Science and Technology, CNR, 20125 Milano, Italy;
[*] See the author list of "Overview of T and D-T results in JET with ITER-like wall" by CF Maggi et al. to be published in Nuclear Fusion Special Issue: Overview and Summary Papers from the 29th Fusion Energy Conference (London, UK, 16-21 October 2023)

Email: Krassimir.Kirov@ukaea.uk

Abstract

This work studies the influence of RF waves in ICRH range of frequency on fusion alphas during recent JET D-T campaign. Fusion alphas from D-T reactions are born with energies of about 3.5MeV and therefore have significant Doppler shift enabling synergistic interaction between them and RF waves at broad range of frequencies including the ones foreseen for future fusion machines ITER [1] and SPARC [2]. Resonant interaction between RF waves and alphas, also called synergistic effects, will modify the alpha distribution and ultimately will have an impact on alpha orbit losses and heating. Data from JET 3.43T/2.3MA pulses based on hybrid scenario [3], [4], [5] during DTE2 campaign [30] were used for the analysis in this study. The impact of synergistic effects on alpha orbit losses and alpha heating is assessed. Conclusions are based on analysis of experimental data for fast alphas losses, i.e. neutral particle analyser, fast ion losses scintillator detector, Faraday cups, and TRANSP [6] simulations. Experimental data and TRANSP analysis indicate that there are indeed changes is alphas distribution function due to interaction with RF waves. Data from neutral particle analyser show increased ^{4}He flux in the range from few hundred keV up to 800keV for pulses with RF power, while TRANSP clearly shows modifications in fast alphas distribution function for these energies. Data from the scintillator detector and the Faraday cups were compared for pulses with and without ICRH power and versus cases with enhanced alpha losses due to MHD activities. The trends from these diagnostics consistently show no additional alpha losses due to interaction with RF waves. TRANSP predictions for the impact of the synergistic effects on alpha heating show up to 42% increase in alpha electron heating and up to 25% increase in alpha ion heating. These effects however become negligibly small, less than 1%, when alpha heating is compared to total auxiliary hearting power for the investigated JET pulses.

1. INTRODUCTION

Fusion alphas from D-T reactions are born with energies of about 3.5MeV. As they slow-down via collisions and exchange energy with background plasma species, an alpha Distribution Function (DF) covering energy range from the thermal background up to about 3.5MeV will be built up and sustained. In conditions of burning fusion plasma i.e. fuel mixture of D/T≈0.5/0.5, electron density n_e≈1×10^{20}m^{-3} and temperature T_e≈10keV the alpha slowing down time is τ_{se}[s]≈0.37(T_e/10[keV])$^{3/2}$/(n_e/10^{20}[m^{-3}])≈0.37s, while the critical energy of ^{4}He ions is of the order of $E_{cr,4He}$[keV]≈33T_e[keV]≈330keV meaning alphas will be predominantly heating thermal electrons.

Alphas born at 3.5MeV will have an absolute velocity of about 1.3×10^{7}m/s which manifests significant Doppler shift in presence of Radio Frequency (RF) waves in the Ion Cyclotron Resonance Heating (ICRH) frequency range. It has been recognised that for ITER [1] and SPARC [2] alpha/RF wave interaction could be a concern regarding: (*i*) parasitic absorption of ICRH power, (*ii*) enhanced alpha orbit losses and (*iii*) impact on alphas heating efficiency. For ITER's main ICRH heating scenario during the active phase of operation, i.e. ^{3}He minorities with RF frequency of f=52.5MHz, vacuum central toroidal magnetic field of B_{t0}=5.2T and toroidal

refractive index $N_\phi=\pm 27$ fusion born alphas will satisfy wave particle resonance condition at R-$R_0\approx$-1.60m for n=1 resonance [7]. Therefore, one would expect significant synergistic interactions between alphas and RF waves.

While alpha losses due to Toroidal Field (TF) ripple and interaction with MHD modes are well covered in the literature, e.g. [8], [9], [10], [11], [12], [13], there seem to be insufficient research with regard to losses due to interaction with RF waves. This deficiency is even more surprising given the fact that early assessments at TFTR have indicated that expected alpha losses due to interaction with RF waves are of similar order as the ones from locked modes, tearing modes and ELMs and larger than the ones expected from fishbones, table 7 in [14]. The gap in the research in this field could be partially due to lack of experimental data on fusion alpha confinement and interaction with the background plasma. Indeed, the only D-T experiments prior JET 2021 campaign were: TFTR D-T campaign in 1994 [14], [15] and previous JET D-T campaign in 1997 [16]. In the latter, the main focus in ICRH related studies was on exploring various ITER relevant ICRH heating scenarios [17] while synergy between alphas and RF waves was somewhat under-researched. TFTR studies [14], [15], [18], [19] have shown that RF waves can induce alpha losses by heating marginally passing alphas and converting them into marginally trapped particles which then impact on the vessel wall [18], [48]. Calculations of the losses [15] with one-dimensional kinetic integral wave code [20] have indicated that about 5–10% of the RF power input to the plasma is absorbed by the fusion-generated alpha particles, while the measured alpha particle losses have been found consistent with this estimate.

Modelling activities of alpha physics were widely available in the late 80-ies and early 90-ies after large scale implementation of parallel Monte-Carlo (MC) codes in fusion calculations as for instance ORBIT [21], [22], NUBEAM [23], OFMC [24], ASCOT [25]. This largely enabled modelling and assessing alpha heating and alpha orbit losses due to TF ripple and MHD modes. The modelling of the interaction of the alphas with RF waves however required implementing an additional algorithm to account for the synergistic effects between RF waves and resonant alphas. This was only available in recent years, for instance in the framework of ORBIT-RF code coupled with TORIC [26] and AORSA [27] as well as in TRANSP/NUBEAM code coupled to TORIC via so called RF kick operator [28], [29].

Recent D-T experiment at JET in 2021 [30], here referred to as DTE2, have provided a solid basis for studying the interaction of fusion alphas with RF waves. This was possible owing to the significant fusion rates achieved during DTE2, of the order of $2\text{-}4\times10^{18}s^{-1}$, as well as significant ICRH heating power, 4-5MW, applied in these experiments in conditions in which energetic alphas have in-vessel resonances. In addition, diagnostic upgrades prior to the JET 2021 campaign provided several additional fast ion diagnostics, a scintillator probe [31], [32] and Faraday cup array [32], [33], which allowed for having deep insight into alpha losses.

This work studies the interaction between RF waves in ICRH range of frequencies and fusion alphas from the recent JET DTE2 campaign. The impact of this interaction on alpha orbit losses and alpha heating has been assessed. Section 2 provides details of the modelling tools used in the study. It is followed by summary of the experimental setup, description of the pulses used in the analysis and essential diagnostics. Experimental results and observations are discussed in section 4. Summary and conclusions are presented in the final section of this manuscript.

2. DETAILS ON MODELLING TOOLS

The TRANSP [6], [34] code was principally used in the analysis presented here. Alpha Distribution Functions (DFs) were calculated by NUBEAM code [23] which is a computationally comprehensive Monte Carlo code for NBI heating in tokamaks. The RF wave solver for TRANSP is TORIC code [35]. Studying the interaction between RF waves and alphas via TRANSP simulations was feasible only after the implementation of RF kick operator in NUBEAM [28], [29]. In general, the following workflow was adopted in calculating alphas interaction with RF waves: TORIC provides information about RF electric field components and the wave vector for each toroidal mode. RF resonance condition for a given harmonic is then used to calculate the magnetic moment and energy of the resonant particles [28], [29]. Every time an alpha particle passes through the resonance layer it receives a kick in magnetic moment space [36]. The magnitude of the kick is derived from the quasi-linear theory [37], while the stochastic nature of the wave-particle interaction is reproduced by means of Monte Carlo random number for the phase of the gyro-orbit. Studying the impact of RF waves/alpha interactions usually requires a pair of TRANSP simulations: one with and the other without RF kick operator. Comparison between the two runs directly shows the impact of the synergistic effects on alpha DFs and heating.

Alpha losses can be in principle calculated by TRANSP, however, due to relatively good confinement and small amount of lost particles at JET, a large number of MC markers would be required to achieve reasonable spatial and temporal resolution. Running TRANSP with a great number of particles, i.e. exceeding 10^6, has been shown to be computationally inefficient. By choosing to use 32k MC markers for alpha particles in this study a compromise between timesaving TRANSP runs and reasonable level of digital noise in lost particle output has been achieved. At the same time, the spatial resolution of the lost alphas was compromised meaning direct comparison to the lost alpha diagnostics cannot be made. An additional limitation in numerical simulations is due to the fact that TRANSP with TORIC cannot provide an accurate estimate of the ICRH power absorbed by the alphas. The wave solver TORIC code works with Fokker-Planck solver FPP code [38] to provide self-consistent power absorption profiles in TRANSP simulations. FPP code is a bounce-averaged zero-orbit width code which for lighter and/or less energetic ions, e.g. minorities and NBI fast ions, is a reasonable approximation. For energetic alphas with significant orbit drifts and banana widths, however, this approximation is crude. TORIC code itself also uses great simplification, bi-Maxwellian DF, in representing alphas and other fast ion species in wave dispersion relation. For the wave solver, however, this approximation should be adequate [35], [39] and able to provide with reasonably good quality the wave electric field and perpendicular wave number. These quantities are needed for RF kick operator calculations in MC code NUBEAM. This way one can still use TRANSP and TORIC codes to assess alpha losses and heating due to synergistic effects. The absorption of ICRH power by alphas however cannot be estimated precisely by means of TORIC and FPP codes and therefore it is not discussed here.

3. EXPERIMENTAL SETUP AND DIAGNOSTICS USED IN THE STUDY

JET D-T pulses carried out at 3.43T/2.3MA based on hybrid scenario [3], [4], [5] with D/T mixture of about 0.5/0.5 were used as references for the analysis in this study. This scenario has demonstrated one of the highest fusion performances in JET DTE2 campaign with a relatively large amount, greater than or approximately equal to 60%, of the total neutron rates, R_{NT}, coming from beam-target reactions [3]. Time traces of core electron density and temperatures as well as neutron rates and heating powers by ICRH and NBI for two similar pulses are shown in Fig. 1 a). Electron density by Tompson Scattering (TS) [40], electron temperature by TS and Electron Cyclotron Emission (ECE) [41] diagnostic and ion temperature by Charge eXchange (CX) spectroscopy [42] diagnostic for the two pulses at 9s are shown in Fig. 1 b).

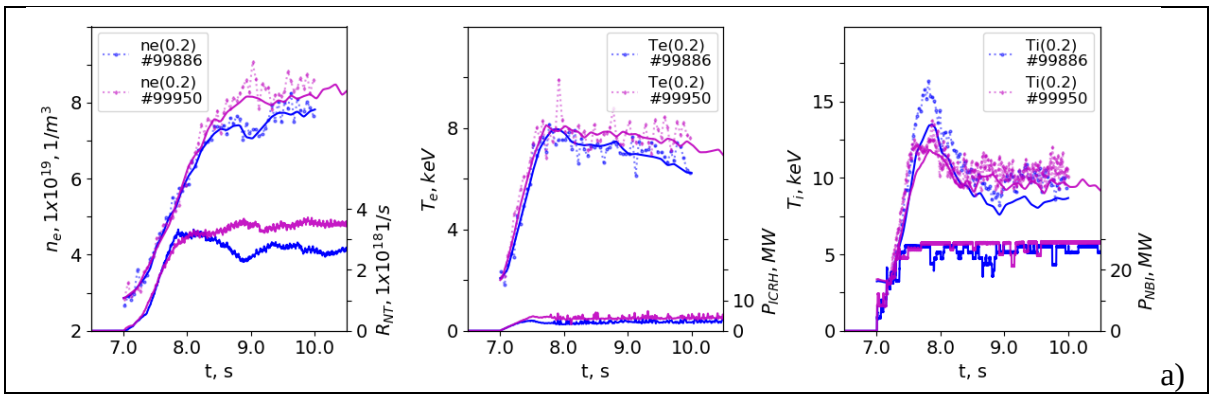

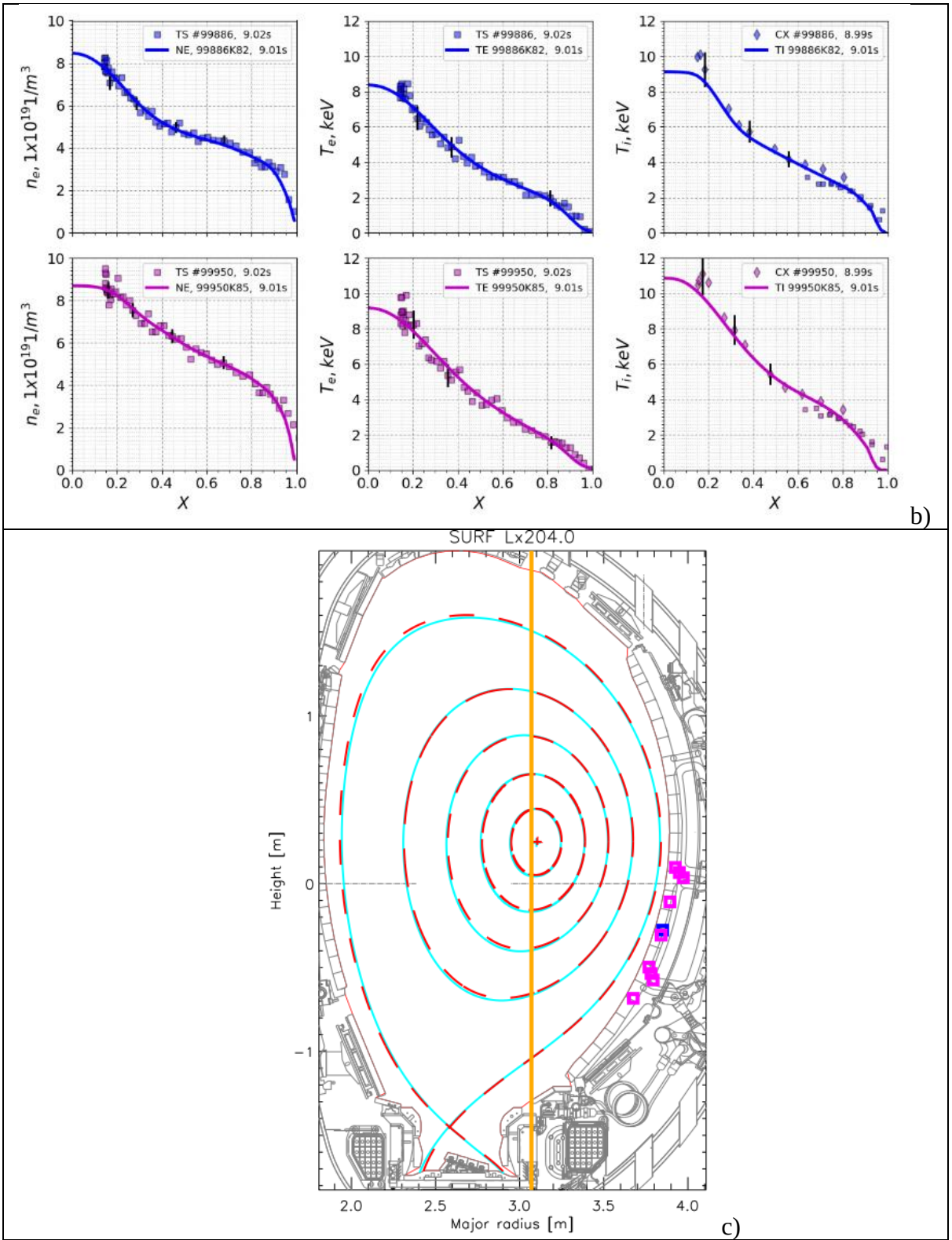

Fig. 1: a) Time traces of electron density n_e and temperature T_e, ion temperature T_i, neutron rates R_{NT} and applied NBI and ICRH power, P_{NBI} and P_{ICRH}, for JET 3.43T/2.3MA hybrid pulses: #99886 with n=2 T ICRH heating scenario (blue) and #99950 in H minority scheme (magenta). b) Profiles of electron density and temperature, ion temperature from the pulses shown in a) at 9s. c) JET cross-section with equilibria from #99802, 8s (dashed red line) and #99950, 8s (cyan line). Shown are approximate positions and line of sight of used diagnostics: Faraday cups (magenta squares for cups #1 to #5 from top to bottom and 3 radial positions of cups #1 and #4); fast ion losses scintillator detector (blue square near Faraday cup #3); neutral particle analyser Line-of-sight (vertical orange line)

While the investigated pulses differ in ICRH heating scenario in general they have very similar time evolution and plasma parameters. In all pulses Neutral Beam Injection (NBI) heating in the range P_{NBI}=25-30MW was applied at 7s after plasma current profile featuring low magnetic shear was formed. This is then accompanied by a transient high-performance phase between 7s and 8s during which beams penetrate deeply in the core in conditions with lower plasma density. ICRH power was ramped up from the same time and P_{ICRH}=3-5MW were sustained during the pulses. Dipole phasing of ICRH antennas which features toroidal refractive index N_ϕ=±27 was used in all experiments reported here.

Different ICRH scenarios were investigated in this study, all summarised in table 1 (see section 4.4), and it was found that in all cases energetic alphas inside plasma boundary are resonant with RF waves. In H minority scenario at B_{t0}=3.43T and f=51MHz, with hydrogen concentration of X[H]=n_H/n_e≈2%, and in pure n=2 D heating, achieved by not injecting H minority, fundamental resonances are at $R_{res,D}$≈1.5m (outside vessel) and $R_{res,H}$≈3.00m. In these conditions alphas in the core are resonant for zero Doppler shift, i.e. for $v_{||}$≈0m/s, with RF waves at 51MHz at n=2 harmonic. For the ITER relevant heating scenario, ^{3}He minority with X[^{3}He]=n_{He3}/n_e≈2-4%, at B_{t0}=3.43T and f=32MHz, and for the corresponding pure n=2 T heating, fundamental resonances are at $R_{res,T}$≈1.6m (outside vessel), $R_{res,D}$≈ $R_{res,He4}$≈2.4m and $R_{res,He3}$≈3.2m. In this case central alphas, i.e. at R≈3.0-3.1m, require Doppler shift of $v_{||}$≈5×10^{6}m/s, to interact with RF waves at 32MHz at fundamental ^{4}He resonance. The fifth scenario investigated here, n=1 D heating, differs in magnetic field, plasma current and D/T mixture [47]: 3.85T/2.5MA, D/T≈0.16/0.84, pulse #99965 in table 1. In these conditions central n=1 D resonance was achieved by applying RF power at 29MHz, which also makes alphas resonant species for zero Doppler shift, i.e. $v_{||}$≈0m/s.

In analysing prompt orbit losses, the initial phase when heating and fusion rates are ramping up is used to compare the trends from lost alphas diagnostics versus neutron rates. In this approach the latter is used as a proxy for alpha source rates. Alpha DF are analysed after approximately 5 slowing down times, i.e. after t=8.5s. In the pulses studied here the q-profile and the start of the heating power were optimized, with broad q>1 region for a long enough period after the start of the heating, so that early MHD activities were avoided [3]. Low amplitude and transient MHD modes were observed but are thought to be benign with regard to fast ion losses. More central n=1 mode followed by fishbone activities which indicate more intense MHD – fast ions interaction appear in one of the investigated pulses, #99950 in time interval 9s<t<10s, and the signals from the lost fast alpha diagnostics in this case were used as an indication of expected trends in conditions with enhanced alpha losses.

A schematic showing the locations and the Line Of Sight (LOS) of the diagnostics used in this study is provided in Fig. 1 c). Neutral Particle Analyser (NPA) [43] is used in addition in pulses where it was set to detect ^{4}He neutrals. LOS of NPA is shown in Fig. 1c).

The scintillator probe [31] is located at the outboard mid-plane, Fig. 1 c), and consists of scintillator plate, CCD and Photo Multiplier Tube (PMT) detector, Fig. 2. The lost fast ions passing through a collimator, Fig. 2 a), impact on the scintillator plate, Fig 2 b), images of which can be recorded via CCD or detected by an array of PMTs. Separation of the fast ion species can be done by assessing the expected Larmour radius and pitch angle from the image on the scintillator [31]. The data discussed here use signals from four PMTs, #10, #11, #14 and #15, which cover the region of the expected lost alphas with Larmour radius between 9cm and 12cm and pitch angles between 55^o and 80^o, Fig 2 b).

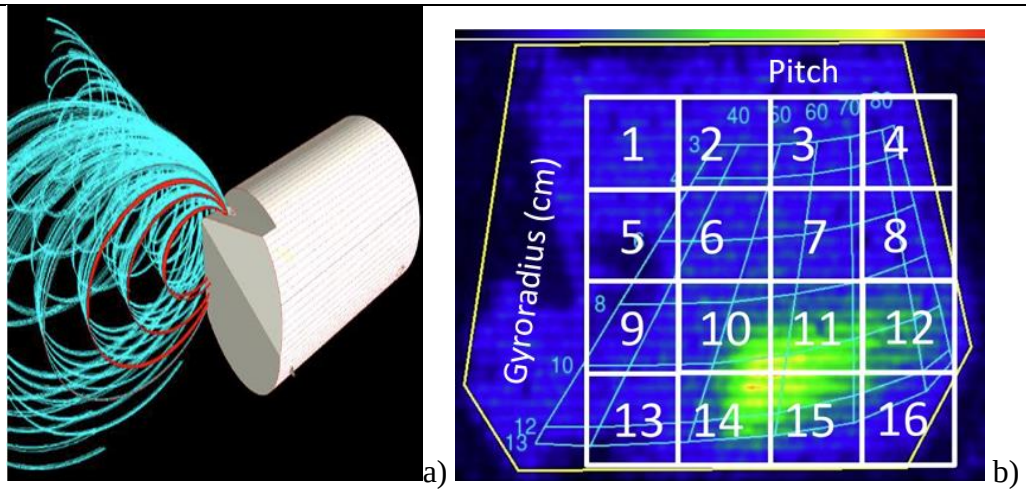

Fig. 2 a) Schematic of lost fast ion scintillator diagnostic in JET with an image of the scintillator plate in b) The observed alpha losses are shown by the green spot and are for Larmor radii between 9cm and 12 cm and pitch angle between 55^o and 80^o. Image is mapped on PMTs numbered #1 to #16, the line of sight of which is shown by white rectangles. Alpha losses for the experiments reported here are detected by PMTs #10, #11, #14 and #15.

Faraday Cups (FC) [32], [33], [44] are an array of five pylons distributed at different poloidal locations as shown in Fig. 1 c) and Fig. 3 a). Each pylon, Fig. 3 b), can contain up to three Faraday Cups foil stacks separated radially. The FC foil stack is composed of four conductive Ni foils separated by mica layers. Lost fast ions will penetrate into the stack and deposit to the foils depending on their energy. The corresponding foil in which a particular ion deposits then will measure the penetrating ion as current. The fast ion energy deposition for various ion species as a function of Faraday cup foil depth can be found in [44]. Fusion alphas in energy range 2.48-3.55MeV are detected by foil 2, data from which is only used here. Separation by species is impossible by FCs so in presence of ICRH power various fast ion species contributions accelerated by RF waves have to be accounted for, e.g. foil 2 also collects fast H minorities in the range 0.68-0.96MeV, as well as D in 0.79-1.10MeV, T in 0.84-1.20MeV and ^{3}He in 2.30-3.35MeV.

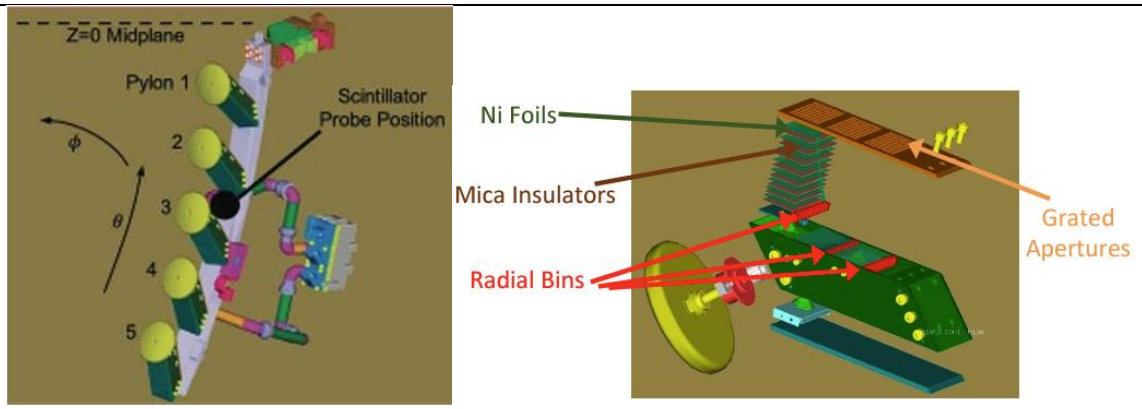

Fig. 3 a) Schematic of FCs array of 5 pylons and schematic of an individual pylon showing the three radial bins and the structure of each stack in b).

4. EXPERIMENTAL RESULTS AND ANALYSIS

An overview of the characteristics of alpha orbits and DF in conditions of JET DTE2 pulses is outlined in the next section.

4.1. Insight into alpha orbits and DF for JET DTE2 pulses

The importance of understanding alpha / RF waves interaction and their impact on alpha losses is firstly outlined here by means of analysis of alpha orbits and DF.

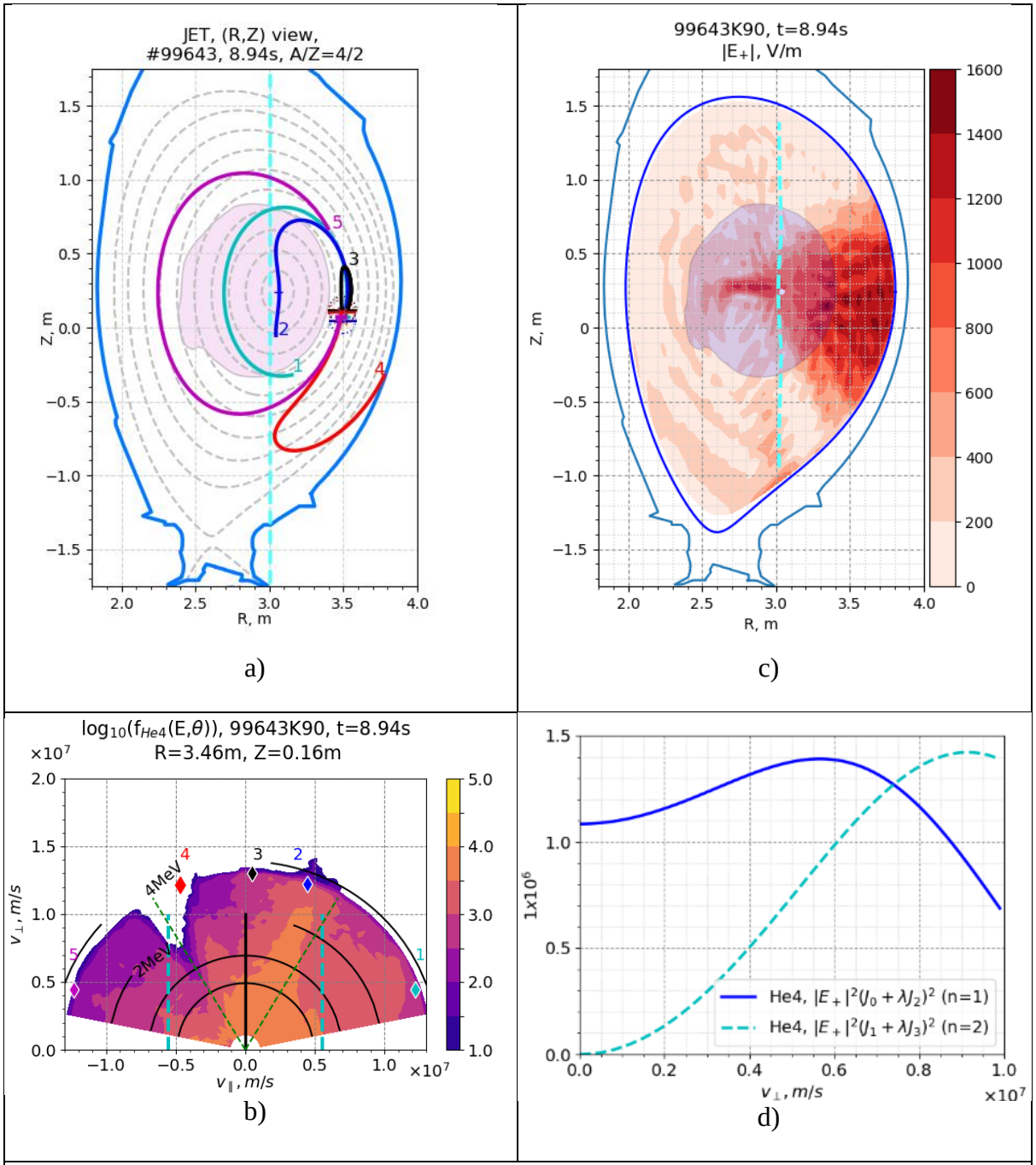

Fig. 4 a) Example of fast alpha orbits for 3.43T/2.3MA JET pulse #99643, 8.94s and particles born at R=3.46m, Z=0.16m with E=3.5MeV and pitch angles of θ=20º (co-passing orbit 1 in cyan) , θ=70º (co-trapped orbit 2 in blue), θ=88º (deep trapped orbit 3 in black), θ=111º (cnt-trapped orbit 4 in red) and θ=160º (cnt passing orbit 5 in magenta). b) Alpha DF at R=3.46m, Z=0.16cm i.e. same location as the starting points of the orbits shown in a). Position of orbits starting points in a) are shown by the corresponding number and colour coded points in b). Also shown in b) by dashed cyan lines are Doppler shifts for n=2 ^{4}He interaction with RF waves with $N_\parallel$=±27 according to eq. (1). RF wave E_+ electric field calculated by TORIC is shown in c). The quasi-linear diffusion coefficient due to RF waves calculated according to eq. (2) for n=1 (solid blue) and n=2 (dashed cyan) is shown in d). Position of n=2 IC resonance for ^{4}He and the region where there are no alpha orbit losses are shown by vertical dashed cyan line and shadowed area in a) and c).

In conditions of JET DTE2 pulses as described in the previous section, i.e. at 3.43T/2.3MA, alphas born in the plasma core, i.e. for toroidal normalised radius of $\rho_t<0.3$, are well confined with regard to orbit losses. The region in which all alpha orbits are confined in the plasma volume is derived by means of TRANSP runs and orbit tracing code and is indicated by shadowed area in Fig. 4 a) and c). The LFS boundary of this area is somewhere between $0.3<\rho_t<0.4$ while on the HFS confined alpha boundary is extended up to $\rho_t\approx0.6$. From TRANSP and orbit tracing code simulations one can deduce the innermost region where alpha orbit losses start to appear, which in our case is on the LFS for $R>3.35$m, $Z\approx Z_{mag}\approx0.25$m, Fig. 4 a). For slightly more peripheral location, i.e. at $R=3.46$m, $Z=0.16$m, Fig 4 shows an example of five alpha orbits in a) and alpha DF in b). From Fig. 4 b) and following the orbit of trapped particle #4, it is clear that the losses in the wedge region of alpha DF around $v_{||}\approx-5\times10^6$m/s will end up on the outer board in the proximity of fast ion losses diagnostics, Fig. 1 c). Cold plasma n=2 resonance for ^{4}He is shown by vertical dashed line at $R\approx3$m in Fig 4 a). For alphas in selected position, i.e. at $R=3.46$m, $Z=0.16$m, to be able to interact with RF waves a significant Doppler shift is required as indicated by dashed cyan lines in Fig 4 b). The latter is derived from wave-particle resonance condition for n=2 and $N_{||}=\pm27$ and taking the local values of magnetic field in the expression for ion cyclotron resonance frequency Ω_{ci}:

$$\omega = n\Omega_{ci} + k_{\parallel}v_{\parallel} \quad (1)$$

In the selected position and at the selected time slice, co-passing (particle #1 in cyan), cnt-passing alpha (particle #5 in magenta) as well as deeply trapped one (particle #3 in black) are non-resonant because of their either too high or too small $v_{||}$. Co-trapped (particle #2 in blue) and cnt-trapped (particle #4 in red) alphas however are resonant as they have the necessary parallel velocity to interact with RF waves despite being away from the IC resonance. In addition, particles #2 and #4 will experience even greater interaction with RF waves as they approach the IC resonance at later stage of their orbit transits and having turning points near the resonance will further intensify this interaction. In the selected location co- and cnt-trapped alphas will experience interaction with RF waves in the form of kick in velocity space, which is proportional to RF induced quasi-linear diffusion coefficient, D_{QL}:

$$D_{QL} \propto |E_+|^2(J_{n-1}(x) + \lambda J_{n+1}(x))^2\ ;\ \lambda = |E_-|/|E_+|\ ;\ x = k_\perp v_\perp/\Omega_{ci} \quad (2)$$

for n=1 and n=2 resonance and combinations of Bessel functions of order n-1, n+1: J_{n-1}, J_{n+1}. The E_+ field of the RF wave is quite strong in selected position on the LFS as provided by TORIC in Fig. 4 c). Therefore, the diffusion in alphas velocity space for n=2 resonance, which is finite Larmour radius effect, depends on particle perpendicular velocity $v_\perp$. Fig. 4 d) shows calculated D_{QL} for n=1 (solid blue line) and n=2 (dashed cyan line) at the selected position, $R=3.46$m, $Z=0.16$m, as a function of alphas $v_\perp$. Clearly the resonant alphas have the necessary $v_\perp\approx0.6$-1.0×10^7m/s for strong interaction with RF waves. This interaction can be even stronger than interaction of resonant thermal ions with RF waves at fundamental frequency as the solid blue line in Fig 4 d) for small $v_\perp$ shows.

Resonant interaction between RF waves and alphas will modify the distribution of the latter and ultimately will have an impact on alpha orbit losses and heating. This has been studied first by means of TRANSP simulations.

4.2. Modifications to alpha DF due to interaction with RF waves

TRANSP calculations of alpha DF for JET 3.43T/2.3MA pulse #99643 with $P_{ICRH}\approx5$MW, $f=51$MHz which in conditions of no H injection gives n=2 central resonance for D and ^{4}He ions, $R_{res,He4}\approx3.00$m, are shown in Fig. 5 a)-d). The position at which alpha DF is analysed, $R=3.08$m, Z=0.21m is selected to be near the magnetic axis where fusion rates are the highest. Fig. 5 b) and the red line in Fig. 5 d) show alpha DF with TRANSP accounting for alpha/RF wave interaction, while Fig. 5 c) and the blue line in Fig. 5 d) show unperturbed DF of alphas, which is achieved by disabling RF kick operator in TRANSP. Significant changes in alpha DF due to interaction with RF waves are predicted for energies up to about 3MeV, while for energies exceeding 3.5MeV impact of RF waves is small as seen from Figs. 5 b), c) and d).

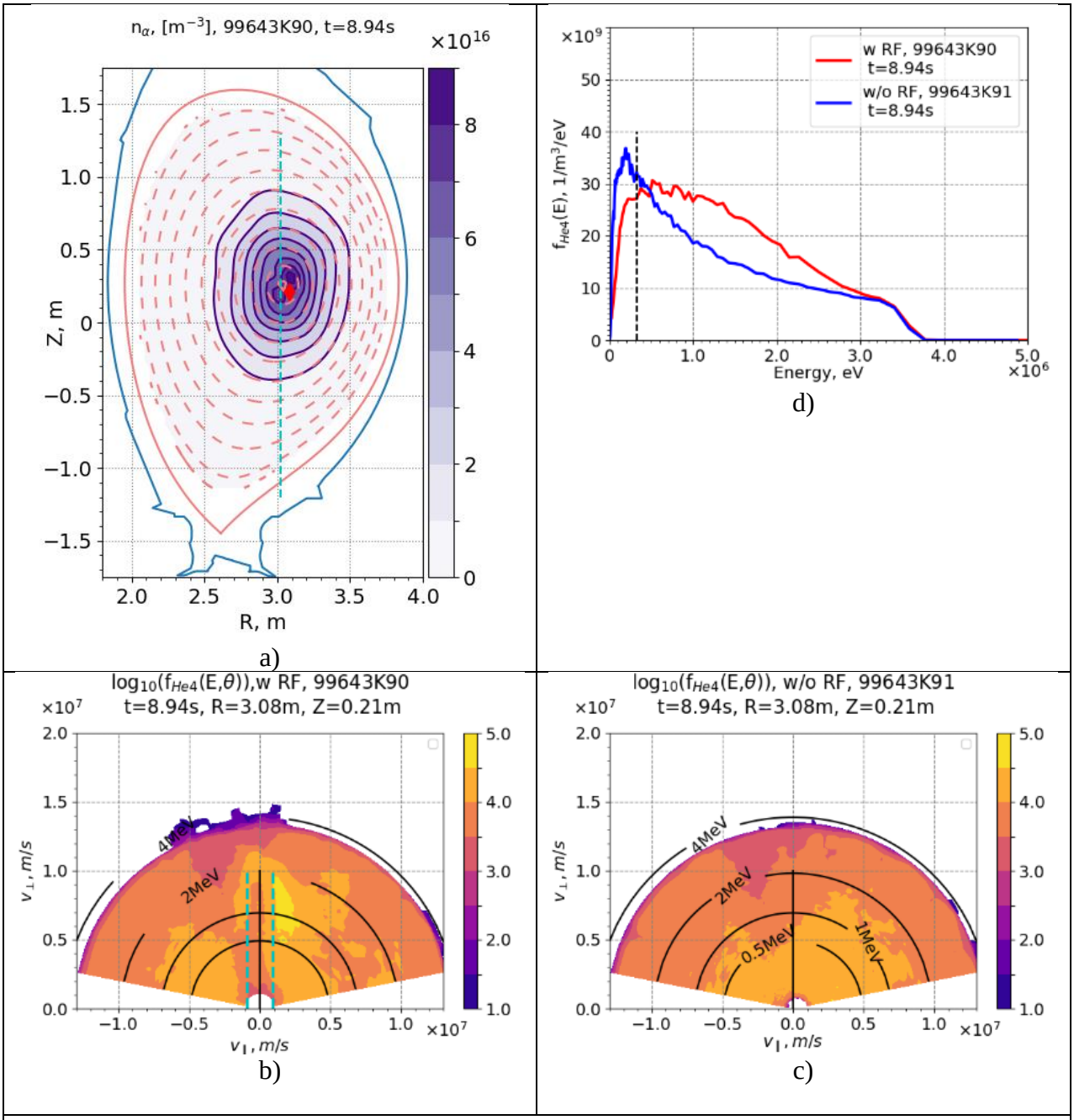

Fig. 5: a) TRANSP output of alpha density during high performance phase of JET D-T pulse #99643 at 8.94s, n=2 D scenario. b) alpha DF log$_{10}$[f(E,θ)] on ($v_\parallel$, $v_\perp$) mesh near the magnetic axis, R≈3.08m, Z≈0.21m from TRANSP run with RF kick operator. c) as b) but for TRANSP run without RF kick. d) alpha DF f(E) near the magnetic axis, R=3.08m, Z=0.21m for the case with (red) and without (blue) RF kick. The position of the cold plasma n=2 ^{4}He resonance is shown in a) by vertical cyan line. Alpha/RF wave interaction for the selected location in b) is affecting particles satisfying wave-particle resonant condition, eq. (1), which for ICRH dipole phasing, N_ϕ=±27, is shown among the dashed cyan lines for n=2 ^{4}He resonance.

TRANSP calculations of alpha DF for JET 3.43T/2.3MA pulse #99886 with P_{ICRH}≈3.5MW, f=33MHz which gives central n=2 resonance for T ions with no minority ^{3}He injection are shown in Fig. 6 a)-d). The fundamental cold plasma ^{4}He resonance in this case is away on the High Field Side (HFS), at $R_{res,He4}$≈2.41m, requiring large Doppler shift for central alphas at R≈3.08m, Z≈0.31m, assessed to be of the order of $v_\parallel$≈5×10^{6}m/s and noted by dashed blue line in Fig. 6 b). Modifications to alpha DF due to interaction with RF waves in this case are lower than in the case discussed in Fig. 5 and mainly for lower energies, up to about 2MeV, Fig. 6 b) and Fig. 6d).

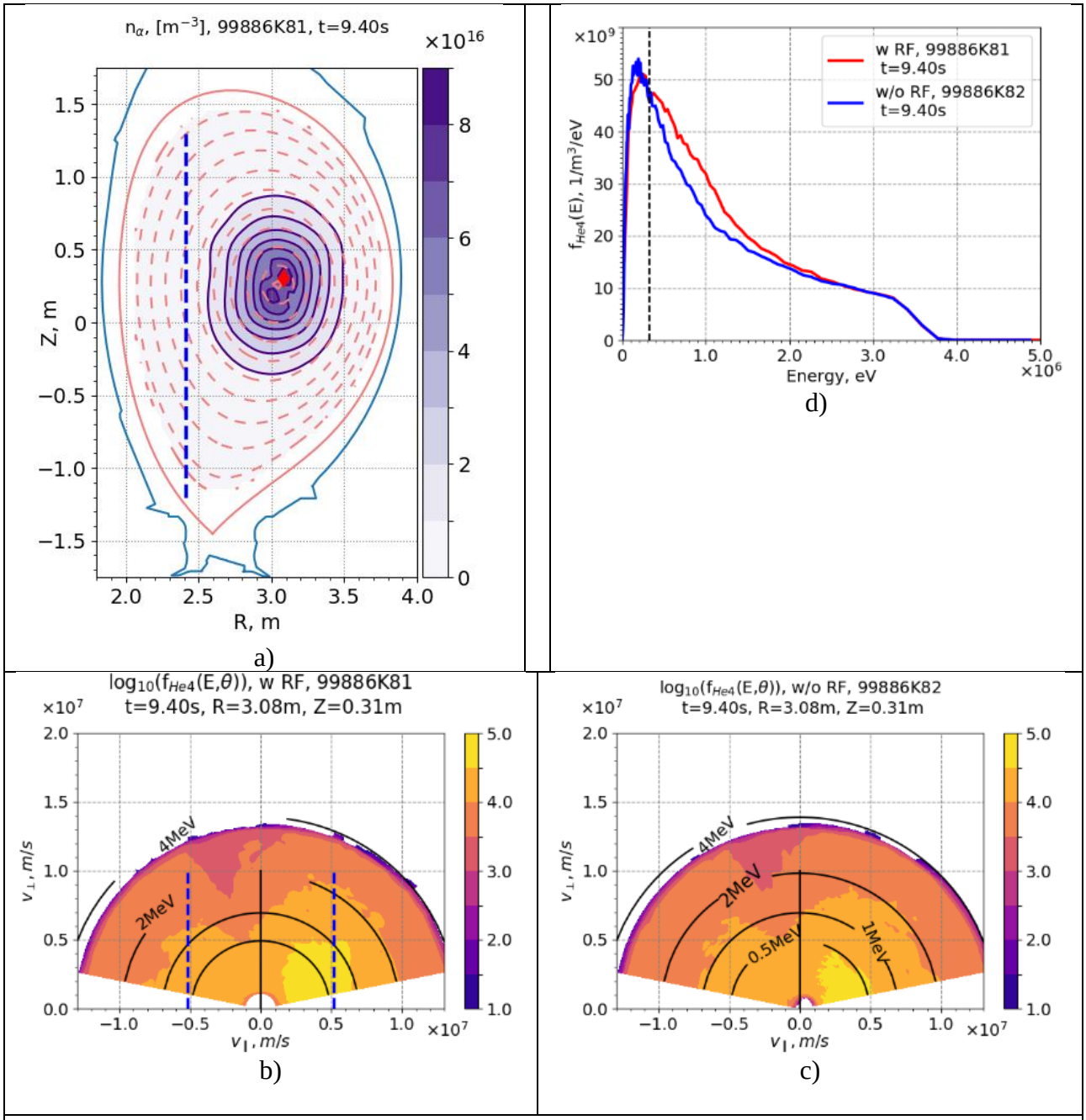

Fig. 6: a) TRANSP output of alpha density during high performance phase of JET D-T pulse #99886 at 9.40s, n=2 T scenario. b) alpha DF $log_{10}[f(E,\theta)]$ on ($v_\parallel$, $v_\perp$) mesh near the magnetic axis, R≈3.08m, Z≈0.31m from TRANSP run with RF kick operator. c) as b) but for TRANSP run without RF kick. d) alpha DF f(E) near the magnetic axis, R=3.08m, Z=0.31m for the case with (red) and without (blue) RF kick. The position of the cold plasma fundamental ^{4}He resonance is shown in a) by vertical dashed blue line. Alpha/RF wave interaction for the selected location in b) is affecting particles satisfying wave-particle resonant condition, eq. (1), which for ICRH dipole phasing, N_ϕ=±27, is shown among the dashed blue lines for n=1 ^{4}He resonance.

Fig. 5 and Fig. 6 clearly show that central alphas can interact with RF waves in both scenarios: n=2 D and n=2 T heating. Modifications to alpha DF due to this interaction are in the range up to 3MeV. No or very negligible acceleration of alphas beyond their birth energy of 3.5MeV is predicted.

4.3. Orbit losses

Central alphas, i.e. in the region 3.0m<*R*<3.1m, are well confined in the investigated JET pulses and TRANSP simulations indicate that no further acceleration exceeding 3.5MeV of the central alphas is expected to take place due to interaction with RF waves. Next step in this investigation is to move outwards towards more peripheral

regions on the Low Field Side (LFS), i.e for R>3.35m for which radius alpha particles' broad banana orbits start to intercept the first wall. Loss cone, which is the region in alpha DF where banana widths are larger than the distance to the wall and consequently particles there experience imminent orbit loss, appears for R>3.35m. For locations further outside on LFS, the loss cone becomes larger. Pulses with central n=2 T resonance, giving $R_{res,He4}$≈2.41m, then would require enormous Doppler shift for alphas on the LFS to have n=1 ^{4}He resonance, while n=2 ^{4}He resonance in this case would be outside the plasma. Pulses with central n=2 ^{4}He resonance however would require reasonable Doppler shift for alphas at locations on the LFS and so these cases are investigated further numerically with TRANSP. Fig 7 shows alpha DF for JET pulse #99643 at two LFS locations with RF kick operator in Fig 7 a) and without RF kick operator in Fig 7 b) for R=3.28m and with RF kick operator in Fig 7 c) and without RF kick operator in Fig 7 d) for R=3.46m.

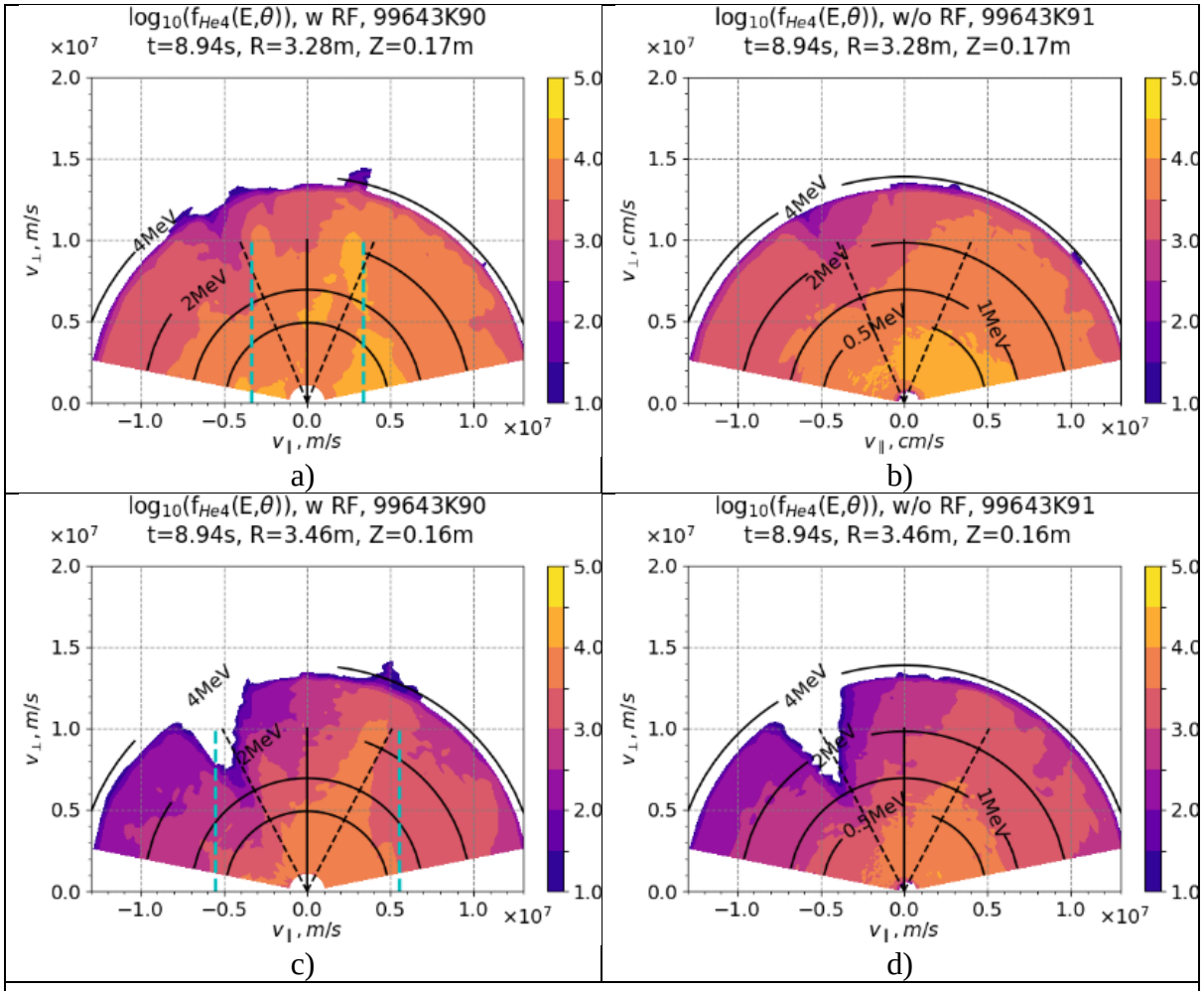

Fig. 7: TRANSP output of alpha DF $log_{10}[f(E,\theta)]$ on ($v_\parallel$, $v_\perp$) mesh at two locations on the LFS for JET D-T pulse #99643, n=2 D scenario. Results in a) are for TRANSP run with RF kick operator at R≈3.28m, Z≈0.17m and in b) for TRANSP run without RF kick operator. Results in c) are for TRANSP run with RF kick operator at R≈3.46m, Z≈0.16m and in d) for same location but without RF kick operator. Shown in a) and c) by vertical dashed cyan lines are parallel velocities required for n=2 Doppler shifted resonance for ICRH dipole phasing, N_ϕ=±27.

Fig. 7 shows that for outboard locations for which R>3.35m the modification of alpha DF due to alpha/RF waves interaction starts to contribute to orbit losses. The two DFs with and without RF kick Fig. 7 a) and b) are at R=3.28m which is the furthest location at which there is no loss cone in alpha DF. The appearance of loss cone is clear at R=3.46m, Z=0.16m location, shown in Fig. 7 c) and d). In both Doppler-shifted resonance locations, $v_\parallel$≈±5.5×10^{6}m/s for $N_\parallel$=±27, RF wave interaction with alphas seem to result in pushing a small number of particles towards higher $v_\perp$. In particular, for $v_\parallel$≈-5.5×10^{6}m/s cnt-passing particles are accelerated towards the loss cone which manifests in enhanced orbit losses, which observation is consistent with TFTR studies [18]. This effect is however very benign on JET as only small modifications to the alpha DF can be seen around the loss cone for $log_{10}[f_{He4}(E,\theta)]$≈1. In addition, the alpha density drops dramatically towards the plasma periphery, cf. $n_\alpha \approx 5.6\times10^{16}$ m^{-3} for the plasma centre, R=3.08m, versus $n_\alpha \approx 3.5\times10^{16}$ m^{-3} for the location at R=3.28m and $n_\alpha \approx$

1.1×10^{16} m^{-3} for R=3.46m. From these simulations one would expect negligible additional orbit losses due to synergistic effects.

TRANSP provides an output for alpha orbit losses by means of rate of total number of lost particles over the whole plasma boundary, noted here as $R_{\alpha,\,loss}$. A more detailed output containing a snapshot of the locations and energies of the lost particles is also available. As discussed in the previous section the detailed spatial analysis would require greater number of MC markers and expensive TRANSP runs therefore it is not used here. TRANSP data for orbit losses, $R_{\alpha,\,loss}$, with and without RF kick operator are shown in Fig. 8.

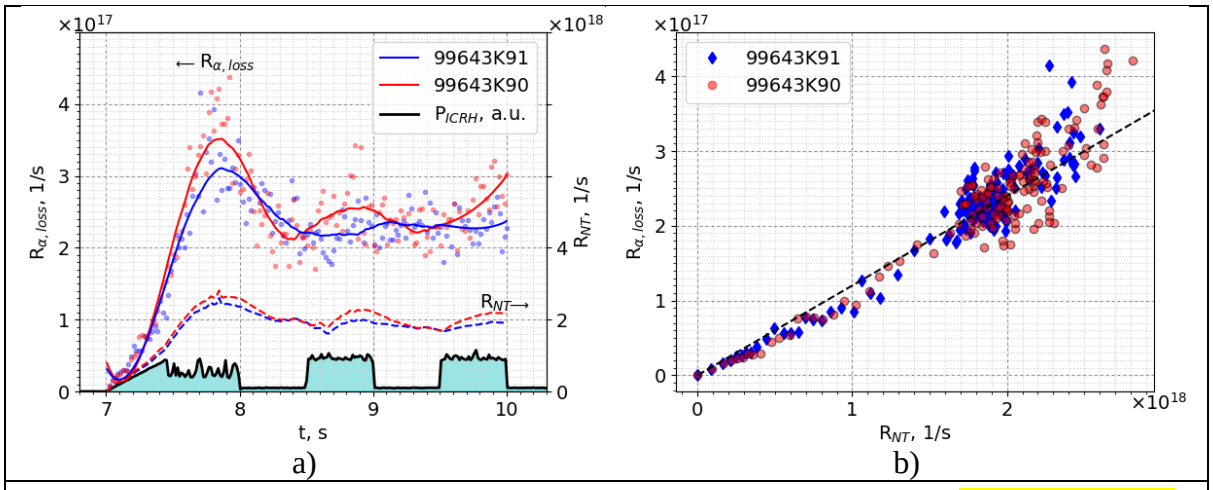

Fig. 8: TRANSP output for time traces of the rate of the total alpha orbit losses, $R_{\alpha,loss}$ (direct output from the code by dots and smoothed lines), and fusion rates, R_{NT}, by dashed lines in a) and alpha losses, $R_{\alpha,loss}$, versus fusion rates, R_{NT}, in b). In a) TRANSP run with RF kick operator is shown by red dots and smoothed solid red line, while run without RF kick operator is noted by blue dots and smoothed solid blue line. In b) same colour code is used for simulations with and without RF kick operator.

Fig. 8 a) shows estimated rates of alpha losses, $R_{\alpha,\,loss}$, over the whole plasma boundary by TRANSP for n=2 D pulse #99643 with and without alpha / RF waves interaction. Although the two TRANSP runs were performed with same input profiles and heating and the only difference being turning on/off the RF kick operator one would also expect difference in fusion performance due to synergy between fast NBI ion and RF waves [45]. Despite the statistical noise due to lower number of MC markers used in these simulations, it can be noted that alpha losses are slightly higher during RF switch on periods in the case with RF kick operator. The observed higher losses are however found to be correlated with the higher fusion rates, i.e. alpha source. This is clearly indicated in Fig. 8 b) where calculated alpha losses, $R_{\alpha,\,loss}$, are plotted versus calculated neutron rates, R_{NT}. In both cases, with and without RF kick operator, the trends approximately follow a straight line for the ratio of lost alphas to created ones of $R_{\alpha,\,loss}/R_{NT}$=0.12 indicated by dashed black line in Fig. 8 b). Based on these simulations it can be concluded that the interaction of alphas with RF waves does not lead to enhanced alpha losses.

The predictions from TRANSP are backed up by experimental observations. JET Neutral Particle Analyzer (NPA) diagnostic can provide experimental verification of alpha particle interaction with RF waves. The analysis of the data from the NPA diagnostic and obtaining more quantitative assessment of the origin and the distribution of the neutrals require additional data processing and modelling of neutrals' transport in plasma. Assessing the birthplace of fast energetic neutrals from JET's NPA data is also challenging due to high densities of these pulses. Fig 9 a) shows measured neutral fluxes of energetic ^{4}He neutrals by NPA for two pulses, with (cyan) and without (red) RF heating. Enhanced losses of ^{4}He particles in the pulse with RF power are observed for energies between ≈600keV and 800keV. One can conclude that TRANSP predictions for the impact of the RF waves on alpha DF are in qualitative agreement with this observation. Indeed, changes in alphas DF for energies between 600keV and 800keV due to RF waves can be clearly seen in Fig. 5 d) and Fig. 6 d).

The lost alphas with energies of about 3.5MeV detected by PMTs in the scintillator detector are analysed and shown in Fig 9 b) and c) versus neutron rates which are taken as a proxy for the alpha source rate. The two diagnostics, PMT and neutron yield monitor, are set up with very different sampling rates, i.e. different time vectors. In the investigated time interval neutrons were sampled with time resolution of ≈6ms, while PMT data was collected at much higher rate between 0.16ms and 0.04ms. The shortest time-scale events discussed here are

the MHD related alpha losses which are usually very transient, ≈0.05-0.1ms, while on the other side neutron rates are expected to evolve on a time scale with energy and particle confinement times as well as with NBI ions slowing down, i.e. at least tens of ms. Based on this assessment, comparing alpha losses on a very short time scale versus neutron rates is done here by interpolating the latter on the PMT time vector which is with much higher time resolution. PMT signal can be in principle processed to give an assessment of alpha losses in terms of physical units, e.g W/m^2, but this requires a complex processing of the data and absolute calibration of the scintillator probe. For the purpose of this study PMT signals from relevant photomultipliers are averaged and provided as a single signal in arbitrary units (AU) which was shown to be proportional to alpha losses [46]. JET pulse with NBI heating only, #99802, 7-7.99s, is used as a reference to indicate the expected dependence of alpha losses on fusion rates in conditions with no ICRH power. The straight line (red diamonds) in this case clearly shows a linear trend of the losses with fusion rates. The expected level of PMT signal for enhanced alpha losses due to MHD are shown (magenta triangles, #99950, 9-10s) for comparison. They are shown as bursts of activities clearly exceeding the expected linear trends. In addition, in Fig. 9 c) shown are alpha losses in quiescent periods between fishbones (black starts, #99950, 9.46-9.47s) indicating slightly lower, but in general level of losses similar to the reference case #99802. The measured trends for pulses with central n=2 ^{4}He resonance, #99950 H minority and #99643 n=2 D as well as #99965 with central n=1 ^{4}He resonance. Clearly the former two cases follow closely the linear dependence set by the reference NBI only pulse #99802 and do not deviate from the straight line as the losses in #99950 after 9s due to bursts of MHD activities, Fig 9 b) and Fig. 10 a) bottom. This means that the calculated $R_{\alpha.loss}$ vs. R_{NT} trends, Fig. 8 b), are consistent with the experimental data and no additional alpha losses were seen in the investigated RF pulses with n=2 central resonance. As for the case with central n=1 ^{4}He resonance, #99965, trends still follow straight line but with a lower slope. This observation is fully consistent with better confined alphas at higher plasma current. The impact of the RF waves in this case however is difficult to assess as there were no reference pulses without ICRH power to compare against. Similar trends were observed for pulses with central T resonance, Fig. 9 c). Both cases, #99634 with ^{3}He minority and #99886 with n=2 T heating indicate no deviation from expected dependence of the alpha losses on the fusion rates.

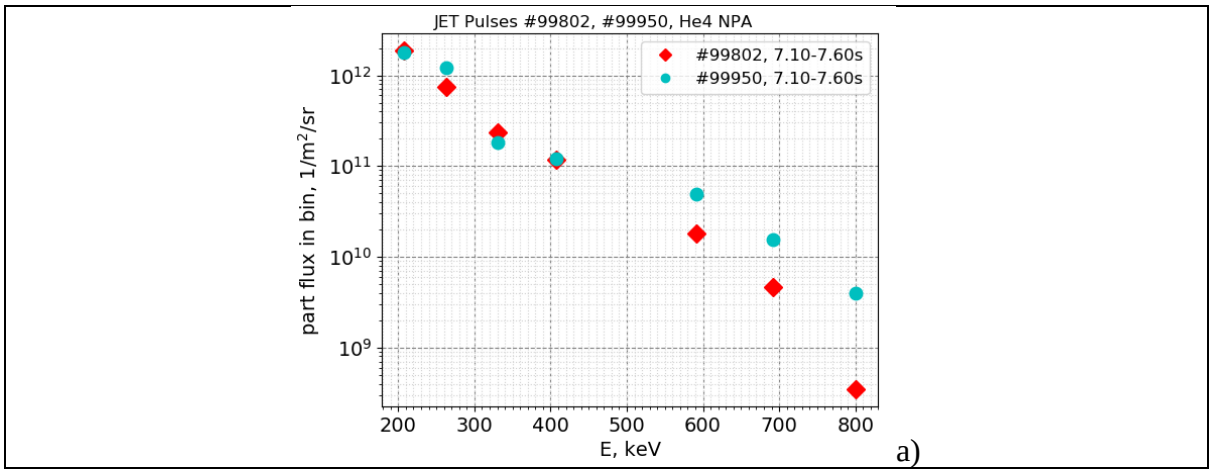

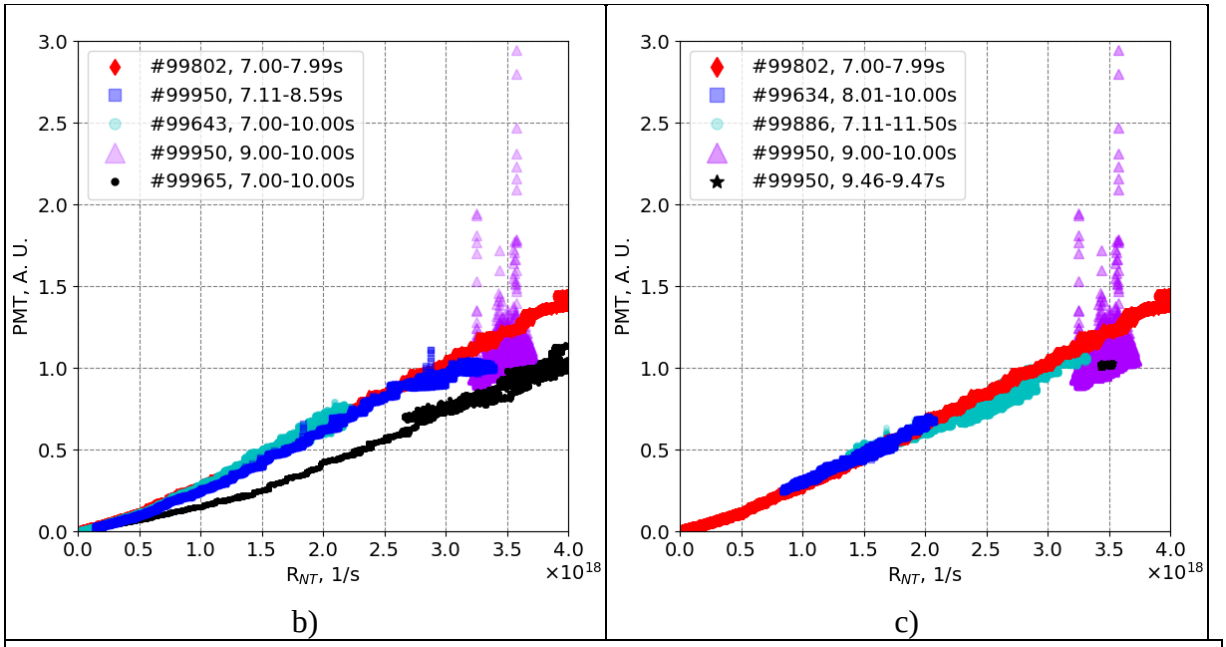

Fig. 9: a) Losses of energetic ^{4}He particles detected by NPA in energy range 200keV to 800keV for JET D-T pulse with ICRH #99950 (cyan) and #99802 without ICRH power (red). In b) and c) shown are fast alpha losses for energies of ~3.5MeV from scintillator probe diagnostics PMT signal versus total neutron rates. Reference pulse is #99802, 7-7.99s, without RF power (red diamonds). Typical increase in PMT signal as a result of alpha losses in #99950, 9-10s, due to MHDs (magenta triangles) is shown for comparison. In addition in b) shown are trends for three different ICRH scenarios: H minority #99950, 7.11-8.59s, (blue squares), n=2 D #99643, 7-10s, (cyan diamonds) and n=1 D #99965, 7-10s, (black points). In c) shown are two different ICRH scenarios: He3 minority #99634, 8-10s, (blue squares) and n=2 T #99886, 7.11-11.50s (cyan diamonds) as well as data for alpha losses in quiescent periods between fishbones, #99950, 9.46-9.47s, (black stars).

Time traces of heating power, neutron rates, signals from FCs 2 and 3 foil 2 and averaged signal from PMT from loss ion scintillator detector for #99950 and #99643 are shown in Fig. 10 a). Signals from FCs are usually very noisy so a simple moving average is applied to them. The low frequency modulations seen on PMTs and FCs in #99643 are correlated with P_{ICRH} as well as with the neutron rates. The data from FCs are again plotted versus neutron rates, R_{NT}. Similarly to Fig. 9 this is done for the signals from FC 3 foil 2 for the pulses discussed above. Here again a pulse without ICRH power, #99802, was used as a reference. As for the case in which enhanced alpha losses due to MHD activities were observed by scintillator detector PMT, #99950, 9-10s, see Fig. 9 b) and Fig 10 a), it was noted that the noise in the data from FCs does not allow for detection of alpha losses due to MHD. Indeed, the time scale for the latter is not sufficiently long for the smoothed FC signals. In addition, significant contribution to FCs noise is due to fast minority ions accelerated by IRCH, cf. reference without ICRH power #99802 with very smooth dependence of FCs on R_{NT}. This means that no proper reference with excessive alpha losses was available for FCs data analysis and therefore only comparison versus losses observed in #99802 is discussed here.

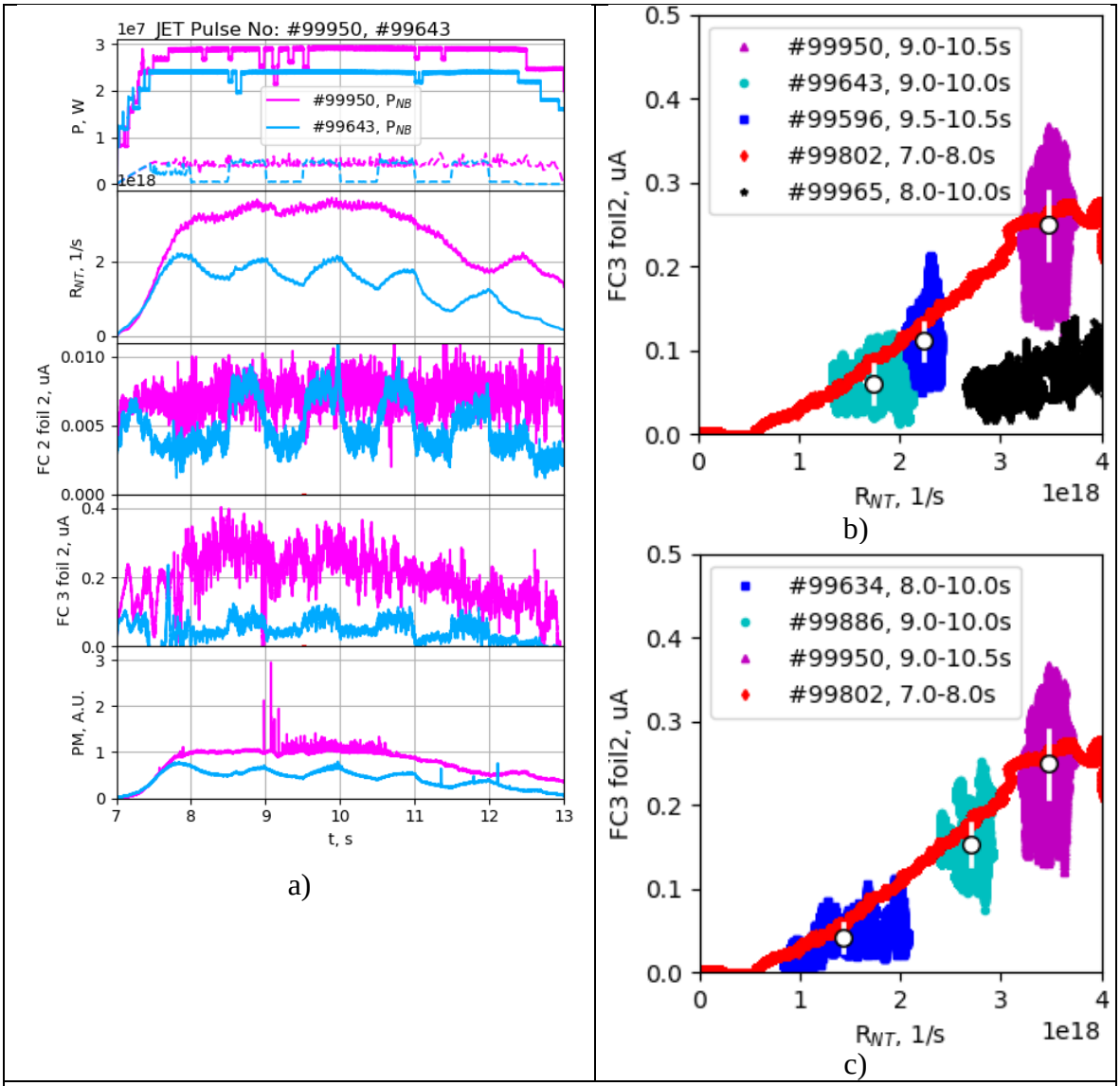

Fig 10. a) Time traces of heating, P_{NB}, P_{RF}, neutron rates, R_{NT}, signals from FC2 foil 2 and FC3 foil 2 and averaged signal from photo multiplier, PMT, from loss ion scintillator detector for #99950(magenta) and #99643(cyan). b) and c) FC3 foil 2 data versus measured neutron rates, R_{NT}. Reference #99802 (red) without ICRH power and #99950 (magenta triangles) in time interval when enhanced alpha losses due to MHDs were observed. In b) signals from #99643 (cyan diamonds) n=2 D ICRH scheme, #99950 (blue squares) H minority and #99965(black points) n=1 D ICRH scheme are shown with their averaged values and standard deviations in white. In c) #99886 (cyan diamonds) with n=2 T ICRH scheme and #99634 (blue squares) with ^{3}He minority ICRH heating are shown with their statistical averages and deviations in white.

Faraday cups data are approximately linear with neutron rates for the reference pulse without ICRH power, #99802. The observed trends for this pulse are consistent with fast ion loss scintillator probe. The noise in pulses #99886 (blue) and #99950 (cyan) and relatively clear linear dependence for #99802 (red) can be explained with the fact that the latter pulse, #99802, does not feature ICRH. Indeed, for the pulses with ICRH power, i.e. #99886 and #99950, a large number of fast H, D and T ions as well as alpha particles are expected to be generated, which would affect the FC measurements. In pulses with sole NBI power only alphas are expected to impact on FC measurements hence the clear linear dependence on the fusion rate. The trends in Fig 10 b) and c) clearly show that FCs signals follow the linear dependence set by the reference case #99802. The noise in FC data due to all other fast ions generated by ICRH was further processed statistically: averaged and standard deviations calculated and shown in Fig. 10 by white symbols and lines. Clearly all data from FC signals stay within the error bars below the reference case #99802. Based on these observations it can be concluded that data from FC also show no indication of enhanced alpha losses due to interaction with RF waves.

4.4. Impact on alpha heating

Alpha heating of electrons was unambiguously observed during DTE2 [49] and is therefore considered an experimentally-verified phenomenon. The observed changes in alpha DF due to synergistic interaction with RF waves are expected to have an impact on alpha heating efficiency as well. Figs. 5 d) and 6 d) clearly show that modification of alpha DF in the region of ^{4}He critical energy, i.e. in our conditions $E_{cr,He4}$≈330keV noted by dashed vertical line, which manifests changes in the electron and ion heating efficiencies of alphas. This is further studied here by means of TRANSP simulations. Similar runs with and without RF interaction are compared with regard to the alpha heating profiles. Power transfer to both species, electrons and ions, in all investigated scenarios has been studied and results are summarised in Table 1.

TABLE 1. Impact of RF waves – alpha interactions on alpha's heating of electrons and ions. All cases are 3.43T/2.3MA D/T≈0.5/0.5 hybrid type of pulses, except for #99965 at the bottom of the table for which pulse details of Bt/Ip and fusion mix are provided. ICRH scenario is listed in column 2. Alpha heating of ions, column 3, and electrons, column 4, are provided by TRANSP with/without RF kick. Second row in columns3 and 4 show total heating power to ions and electrons.

Pulse, time slice of interest	**RF heating scenario, *He4 resonance***	**Alpha heating of ions with/without RF kick, [MW]** ***Total ion heating with/without RF kick, [MW]***	**Alpha heating of electrons with/without RF kick, [MW]** ***Total electron heating with/without RF kick, [MW]***
#99596, 9s	H min X[H]≈2% 51MHz, $R_{res,He4}$≈*3.02m (n=2)*	0.10/0.08 *16.38/16.36*	0.87/0.69 *8.76/8.31*
#99634, 9s	He3 min X[He3]≈2% 32MHz, $R_{res,He4}$≈*2.41m (n=1)*	0.08/0.08 *15.37/15.75*	0.69/0.69 *6.35/6.40*
#99643, 9s	n=2 D X[H]=0% 51MHz, $R_{res,He4}$≈*3.02m (n=2)*	0.11/0.09 *16.98/17.02*	1.19/0.84 *8.38/7.06*
#99802, 8s	no RF, reference pulse	-/0.11 *-/18.45*	-/1.23 *-/5.15*
#99886, 9s	n=2 T X[He3]=0% 32MHz, $R_{res,He4}$≈*2.41m (n=1)*	0.13/0.12 *19.87/19.66*	0.94/0.93 *7.25/7.05*
#99950, 9s	H min X[H]≈2% 51MHz, $R_{res,He4}$≈*3.02m (n=2)*	0.22/0.21 *20.26/20.52*	1.61/1.49 *9.65/9.48*
#99965 3.85T/2.45MA T/D~0.84/0.16 9s	n=1 D 29MHz, $R_{res,He4}$≈*3.06m (n=1)*	0.28/0.23 *20.41/19.22*	2.41/2.13 *11.45/10.52*

In all cases of interest alpha heating is split between electron and ions in an average ratio of about 0.89/0.11. Table 1 shows that alphas electron heating was in the range 8-16% of the total electron heating for the 3.43T/2.3MA scenarios and 20% in n=1 D heating scenario, #99965. At the same time alphas heating of ions is negligible and only account for 0.5-1.2% of the total ion heating.

An interesting observation is that while alpha electron heating changes due to synergy effects, the ion heating is practically not affected. To a certain extent this is not surprising given that alpha heating on ions is very modest and the alpha DF is mainly affected for larger energies, E>500keV. With critical energy of ^{4}He in D/T mixture for JET conditions with T_e≈10keV of about $E_{cr,He4}$≈330keV the changes in alphas DF due to synergistic effects, Fig. 5 d) and 6 d), are expected to mainly impact electron heating.

Analysis of the alpha heating with and without synergistic effects is discussed here on the basis of (*i*) changes in alpha heating and (*ii*) impact on the total heating. Changes in alpha heating due to RF wave / alpha interaction are not small: alpha heating of electrons varies and increases by up to 42% due to RF induced changes in alpha DF, while for ions one gets up to 25% increase. When this is translated into contribution to total electron and ion heating, second lines in table 1, the figures are much smaller: typically, one sees an increase of alphas electron heating within 1% of total electron heating. The changes in alphas contribution to total ion heating due to synergistic effects are even smaller, less than 0.2% of the total ion heating power.

5. DISCUSSION AND CONCLUSIONS

The analysis reported here provides further insight into the consequences of RF waves – alpha interaction expected to take place in future fusion devices. In conditions as in JET DTE2 hybrid type pulses with fusion rates of 2-$4\times10^{18}s^{-1}$ and maximum ICRH power of 4-5MW all five ICRH scenarios listed in table 1 have ^{4}He resonances in the plasma. In all five cases energetic alphas have sufficient energy, i.e. Doppler shift and perpendicular momentum, to interact effectively with RF waves. Results of this study show that there are moderate changes in the alpha DF due to this interaction. Experimental data show increased ^{4}He flux for energies from few hundred of keV up to 800keV for pulses with RF power, while TRANSP clearly shows modifications in fast alpha DF in this energy range. This however seems to have negligible impact on alpha losses. Data from lost ion scintillator detector and Faraday cups consistently show no excessive alpha losses due to RF waves. TRANSP estimates of the losses are consistent with the experimental observations: linear increase of total alpha losses to fusion rates with a slope of $R_{\alpha,\,loss}/R_{NT}$=0.12 was derived for the cases with and without RF kick operator.

Changes in alphas electron and ion heating due to RF waves / alpha interactions were studied by means of TRANSP simulations with and without RF kick. The predicted increase in alphas electron heating due to the synergistic effects is relatively small when compared to total electron heating, but it can reach up to 42% if alpha electron heating only is considered. For ions alpha heating is negligible with regard to total ion heating, while alpha ion heating itself is found to increase by max of about 25%. These figures therefore are important for devices which would rely heavily on alpha heating, in particular future reactors designed to operate close to "burning plasma" conditions, while for JET with dominant auxiliary heating the changes are small.

An interesting observation at JET, which seem to be inconsistent with TFTR observations is that alpha losses due to interaction with RF waves are lower than the losses caused by fishbones. Indeed, according to table 7 in [14] alpha losses due to interaction with RF waves are expected to be 4 times higher than the ones by fishbones in TFTR. In JET conditions however Figs. 9 b) and c) and Fig. 10 a) show that the fishbone losses prevail. A possible explanation of this observation could be due to different ripple in these two devices. TFTR is with fewer number of TF coils than JET and therefore alpha losses in TFTR are more affected by the comparatively larger TF ripple. As a consequence of this alpha interaction with RF waves resulting in radial displacement would result in more ripple losses in TFTR conditions compared to JET.

ACKNOWLEDGEMENTS

This work has been carried out within the framework of the EUROfusion Consortium, funded by the European Union via the Euratom Research and Training Programme (Grant Agreement No 101052200 — EUROfusion). Views and opinions expressed are however those of the author(s) only and do not necessarily reflect those of the European Union or the European Commission. Neither the European Union nor the European Commission can be held responsible for them.

REFERENCES

[1] [1] Schneider M. et al, Nucl Fusion 61 126058 (2021).
[2] [2] Creely A. J. et al, J Plas Phys, vol 86, 865860502 (2020)
[3] [3] Hobirk J. et al, Nucl Fusion, special issue (2023)
[4] [4] Hobirk J. et al, 29th IAEA FEC23 conference, London, UK, 16-21 Oct 2023
[5] [5] Challis C. D. et al, 48th EPS Conference on Plasma Physics, 27 June - 1 July 2022.
[6] [6] Hawryluk R. J. et al, An empirical approach to tokamak transport Physics of Plasmas Close to Thermonuclear Conditions Vol, 1, ed B. Coppi et al (Brussels: CEC) pp 19–46; DOI 10.11578/dc.20180627.4 (1980)
[7] [7] Budny R. V., Gorelenkova M., 57th Annual Meeting of the APS Division of Plasma Physics, Volume 60, Number 19, GP12.00127 (Savannah, Georgia, 16–20 Nov 2015) (2015)
[8] [8] Fasoli A. et al, Nucl Fusion 47, S264 (2007)
[9] [9] ITER physics, Nucl. Fusion 39, 2471 (1999)
[10] [10] Sharapov S. E. et al, Nucl. Fusion 39, 373 (1999)
[11] [11] Kiptily V. et al, 29th IAEA FEC23 conference, London, UK, 16-21 Oct 2023
[12] [12] Bonofiglo P. J. et. al, 29th IAEA FEC23 conference, London, UK, 16-21 Oct 2023

[13] [13] Garcia J. et al, 29th IAEA FEC23 conference, London, UK, 16-21 Oct 2023
[14] [14] Zweben S.J. et al, Nucl. Fusion 40, 91 (2000)
[15] [15] Taylor G et al, Plasma Phys. Control. Fusion 38, 723 (1996)
[16] [16] Jacquinot J. et al, Nucl Fusion 39, 235 (1999)
[17] [17] Start D. et al, Nucl Fusion 39, 321(1999)
[18] [18] Darrow D.S. et al, Nucl. Fusion 36, 1 (1996)
[19] [19] Lam N. T. et al Nucl. Fusion 34 1161 (1994)
[20] [20] Sauter O. and Vaclavik J., Nucl. Fusion 32, 1455 (1992)
[21] [21] Redi M.H. et al, Nucl. Fusion 35, 1509 (1995)
[22] [22] White, R.B., Chance, M.S., Phys. Fluids 27, 2455 (1984)
[23] [23] Pankin A., McCune D., Andre R. et al., "The Tokamak Monte Carlo Fast Ion Module NUBEAM in the National Transport Code Collaboration Library", Computer Physics Communications Vol. 159, No. 3, 157-184 (2004)
[24] [24] Tani K. et al, J Phys Soc Japan 50, 1726 (1981)
[25] [25] Hirvijoki E. et al. Comput. Phys. Commun. 185, 1310 (2014)
[26] [26] Choi M. et al, Phys Plasmas 12, 072505 (2005)
[27] [27] Choi M. et al, Phys Plasmas 17, 056102 (2010)
[28] [28] Kwon J.-M. et al, 48th meeting of the Division of Plasma Physics, Philadelphia (PA) (2006);
[29] [29] Kwon J.-M. et al, 49th meeting of the Division of Plasma Physics, Orlando (FL) (2007).
[30] [30] Maggi C. F. et al, Nucl Fusion special issue (2023)
[31] [31] Baeumel S. et al, Rev. Sci. Instrum. 75, 3563 (2004)
[32] [32] Darrow D. et al, Rev. Sci. Instrum 77, 10E701 (2006)
[33] [33] Darrow D. et al, Rev. Sci. Instrum 75, 3566 (2004)
[34] [34] Grierson B. A. et al "Orchestrating TRANSP Simulations for Interpretative and Predictive Tokamak Modeling with OMFIT", Fus. Sci. Techn. (2018)
[35] [35] Brambilla M., Plasma Phys. Control. Fusion 41, 1 (1999)
[36] [36] Stix T. H., Nucl. Fusion 15 737 (1975)
[37] [37] Kennel C. F., Engelmann F., Phys Fluids, vol 9, 2377 (1966)
[38] [38] Hammett G.W., "Fast Ion Studies of Ion Cyclotron Heating in the PLT Tokamak", Ph.D. Thesis (Princeton, 1986)
[39] [39] Bilato R. et al, Nucl Fusion 51, 103034 (2011)
[40] [40] Gowers C. et al, Rev. Sci. Instrum. 66, 471 (1995)
[41] [41] de la Luna E. et al, Rev. Sci. Instrum. 74, 1414 (2001)
[42] [42] Biewer T.M. et al, “Charge Exchange Recombination Spectroscopy Measurements from Multiple Ion Species on JET”, JET report EFDA–JET–CP(07)03/24 (2007)
[43] [43] Korotkov A. A. et al, Nucl. Fusion 37, 35 (1997)
[44] [44] Bonofiglo P. J. et. al Rev. Sci. Instrum. 91, 093502 (2020)
[45] [45] Kirov K. K. et al Nucl Fusion, accepted, (2023)
[46] [46] Rivero-Rodriguez J.F. et al, Rev. Sci. Instrum. 92, 043553 (2021)
[47] [47] Maslov M. et al Nucl Fusion special issue (2023)
[48] [48] Chang C. S. Phys Fluids28 3598 (1985)
[49] [49] Kiptily V. G. et al Phys Rev Letters 131 075101 (2023)